Generalized oscillator strengths for some higher valence-shell excitations of argon

Lin-Fan Zhu,* Hui Yuan, Wei-Chun Jiang, Fang-Xin Zhang, Zhen-Sheng Yuan, Hua-Dong Cheng, and Ke-Zun Xu
Hefei National Laboratory for Physical Sciences at Microscale, Department of Modern Physics, University of Science and Technology of China, Hefei, Anhui, 230026, China

(Received 29 November 2006; revised manuscript received 4 February 2007; published 5 March 2007)

The valence shell excitations of argon were investigated by an angle-resolved fast-electron energy-loss spectrometer at an incident electron energy of 2500 eV, and the transition multipolarities for the excitations of $3p \rightarrow 3d$, $4d$, $5s$, and $5p$ were elucidated with the help of the calculated intermediate coupling coefficients using the COWAN code. The generalized oscillator strengths for the excitations to $3p^5(3d,3d')$, $3p^5(5p,5p')$, and $3p^5(5s,4d)$ were measured, and the profiles of these generalized oscillator strength were analyzed. Furthermore, although the present experimental positions of the maxima for the electric-monopole and electric-quadrupole excitations in $3p \rightarrow 5p$ are in agreement with the theoretical calculations [Amusia *et al.*, Phys. Rev. A **67**, 022703 (2003)], the generalized oscillator strength profiles show obvious differences. In addition, the experimental generalized oscillator strength ratios for the electric-octupole transitions in $3p \rightarrow 3d$ are different from the theoretical prediction calculated by the COWAN code.

DOI: 10.1103/PhysRevA.75.032701 PACS number(s): 34.80.Dp, 34.80.Gs, 33.70.Fd, 31.15.Ne

I. INTRODUCTION

For noble gases of Ne, Ar, Kr, and Xe, their excited energy level structures are well described by intermediate coupling, while their ground states are closed-shell $^1S_0$ states of *LS* coupling, so noble atoms are typical systems to study the valence-shell excitation mechanism and dynamics relating to two different coupling schemes [1–3]. There are also tremendous challenges for theoretical models because of the complications of many-electron atoms and the non-*LS*-coupling nature of argon. Furthermore, the generalized oscillator strengths (GOS's) can be used to evaluate the theoretical methods, determine the correct spectral assignments [4], and explore the excitation dynamics [5]. The deviation of the magnitudes and positions of the minima or maxima of GOS's predicted by the theoretical calculations from the experimental results will serve as a test of the applicability of the Born approximation as well as the accuracy of the wave functions [6]. And the study of GOS's for the valence-shell excitations of argon is of great importance in many areas such as astrophysics, discharge process, plasma physics, laser physics and etc. [7,8].

We have been continuing investigations of GOS's and differential cross sections (DCS's) for valence-shell excitations of noble atoms (He [9], Ne [2], Ar [3], Kr [10]) by fast electron impact. In this work, as an addition to our previous measurements of the GOS's for the excitations to $3p^5(4s,4s',4p,4p')$ in Ar [3] (referred to from now as paper I), we present the GOS's for higher valence-shell excitations to $3p^5(3d,3d')$, $3p^5(5p,5p')$, and $3p^5(5s,4d)$.

There are many experimental measurements [3,11–21] and theoretical calculations [18,22–26] of GOS's and DCS's for the valence-shell excitations of Ar, which were summarized in paper I. However, most of the previous works were carried out with low incident electron energies [11–16]; the measured GOS's were only limited to the transitions to $3p^5(4s,4s')$ and $3p^5(4p,4p')$ [3,17–21]. To the best of our knowledge, only Amusia *et al.* [26] calculated the GOS's for the electric-monopole and electric-quadrupole excitations in $3p \rightarrow 5p$ using the Hartree-Focrk (HF) and random phase approximation with exchange (RPAE) methods.

With the above survey, most of previous works were carried out with low incident electron energies, in which the transitions between states with different spin multiplicities are possible as a result of electron exchange effects [27]. For sufficiently fast electron impact, the influence of the incident particle upon an atom or molecule can be regarded as a sudden and small external perturbation. Thus the cross section can be factorized into two factors, one dealing with the incident particle only, the other (GOS) dealing with the target only, and the exchange effect is negligibly small [27]. The GOS was defined as [27–29] [in atomic units (a.u.)]:

$$f(E,K) = \frac{E}{2}\frac{p_0}{p_a}K^2\frac{d\sigma}{d\Omega} = \frac{2E}{K^2}\left|\langle\Psi_n|\sum_{j=1}^{N}\exp(i\mathbf{K}\cdot\mathbf{r}_j)|\Psi_0\rangle\right|^2, \quad (1)$$

where E is the excitation energy, K is the momentum transfer, and p_0 and p_a are the incident and scattered electron momenta, respectively. $f(E,K)$ and $d\sigma/d\Omega$ stand for GOS and DCS while Ψ_0 and Ψ_n are N-electron wave functions for initial and final states, respectively. $\mathbf{r}_j$ is the position vector of the jth electron.

In the present work, the GOS's for the higher valence-shell excitations to $3p^5(3d,3d')$, $3p^5(5p,5p')$, and $3p^5(5s,4d)$ of Ar were measured at an incident electron energy of 2500 eV. The GOS profiles for these excitations were analyzed, and their momentum positions of maxima were determined. The transition multipolarities for these excitations were elucidated with the help of our calculated intermediate coupling coefficients using the COWAN code [30].

*Corresponding author. Electronic address: lfzhu@ustc.edu.cn

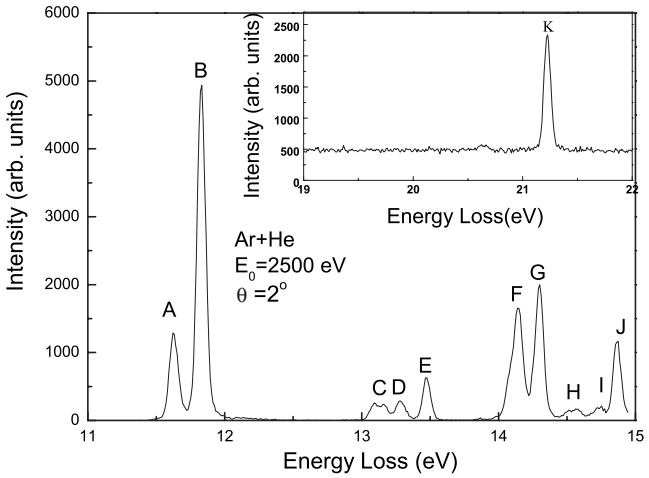

FIG. 1. A typical electron-energy-loss spectrum of Ar+He at the impact energy of 2500 eV and the scattering angle of 2°.

II. EXPERIMENTAL AND THEORETICAL METHOD

A. Experimental method

The experimental method and experimental setup are the same as in paper I, the impact energy was set at 2500 eV, and the energy resolution was 75 meV [full width at half maximum (FWHM)]. A typical electron-energy-loss spectrum is shown in Fig. 1, where the peaks from *A* to *J* are labeled, the excitations from *A* to *E* were analyzed in paper I. The peak *K* corresponds to the excitation to $2\,^1P$ of helium, which is used to calibrate the data. Since every one of peaks *F*–*I* includes several excitations, the intensity for each excitation was determined by least-squares fitting procedure. In the fitting procedure, we assume that all excitations have the same peak profile, which was determined by fitting the first two excitations of $4s[3/2]_1$ (peak *A*) and $4s'[1/2]_1$ (peak *B*), and the energy positions taken from Moore [31] were fixed. As for the excitation to $2\,^1P$ of helium, linear base line was deducted in the fitting procedure. Figure 2 shows deconvolved results of the spectrum at the scattering angle of 2° for the peak *F*, *G*, *H*, and *I*.

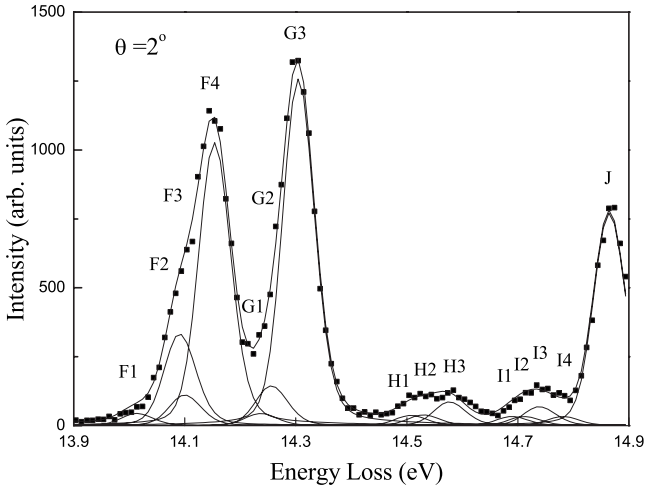

FIG. 2. The deconvolved result of the spectrum for the peaks *F*, *G*, *H*, and *I* at the scattering angle of 2.0°. Solid squares, the experimental data; solid line, the fitted results.

After the intensity for each excitation was obtained, following the same procedure as discussed in paper I, the relative DCS's and GOS's for the transitions in the present measured energy loss region of 13.9–14.8 eV were determined. The relative GOS's for these excitations were converted to absolute GOS's by being multiplied by the same scale factor used to determine the GOS scale for $4s'[1/2]_1$ in paper I. Because the energy resolution is not high enough, we only present the sum of GOS's for the excitations whose energy level intervals are less than 40 meV.

The overall errors in this work come from the statistics of counts δ_s, the angular resolution determination for small angle δ_r, the pressure correction δ_p, and the normalizing procedure δ_n, as well as the error resulting from the deconvolution procedure δ_d. In this work, the maximum of each error is $\delta_s=8\%$ for the weakest transition, $\delta_r=5\%$, $\delta_p=5\%$, $\delta_n=5\%$, and $\delta_d=12\%$. The total errors are less than 17%.

B. Calculational method

The calculations of the intermediate coupling coefficients for the lowest 39 levels of Ar were performed with the COWAN code [30]. The method of calculation was described in detail by Clark *et al.* [32,33], and summarized in paper I and our recent work [2].

For the present calculations, a 36-configuration basis set was used and the calculated excitation energies are consistent with the Moore levels [31] within 0.07 eV. The calculated intermediate coupling coefficients and the energy levels that are involved in the peak *F*, *G*, *H*, and *I* are listed in Table I. The other calculated intermediate coupling coefficients and the energy levels that are involved in the peaks *A*, *B*, *C*, *D*, and *E* have been listed in Table I of paper I.

III. RESULTS AND DISCUSSIONS

From Table I it can be noticed that the excited states of $5s[3/2]_2$, $5s'[1/2]_0$, and $5p[5/2]_3$ only consist of the triplet components in the intermediate coupling scheme. Since the probability for the spin-forbidden transition in connection with the electron exchange effect is negligibly small for fast electron impact [27], the contributions of the excitations from the ground state of $^1S_0$ to the triplet components can be neglected. Thus these excitations were not observed in the present spectra. In addition, the magnetic-dipole excitations to $5p[1/2]_1$, $5p[3/2]_1$, $5p'[3/2]_1$, and $5p'[1/2]_1$, as well as the magnetic quadrupole excitations to $3d[5/2]_2$, $3d'[5/2]_2$, and $3d[3/2]_2$, should not appear in the present spectra based on their singlet components [1,2,34]. Therefore, according to the singlet components shown in Table I, the observed transitions of Ar in our concerned energy region consist of the electric-monopole excitations to $5p[1/2]_0$ and $5p'[1/2]_0$, electric-dipole excitations to $3d[1/2]_1$, $5s[3/2]_1$, $3d[3/2]_1$, $5s[1/2]_1$, $3d'[3/2]_1$, and $4d[1/2]_1$, and electric-quadrupole excitations to $5p[5/2]_2$, $5p[3/2]_2$, and $5p'[3/2]_2$, as well as electric-octupole excitations to $3d[7/2]_3$, $3d[5/2]_3$, $3d'[5/2]_3$, and $4d[7/2]_3$. Herein the intensity of electric-

TABLE I. The intermediate coupling coefficients and the assignments for peaks from *F* to *I*. The energy levels from Moore [31] and from our calculations are listed. E_0, E_1, E_2, E_3, M_1, M_2, and T represent the electric-monopole, electric-dipole, electric-quadrupole, electric-octupole, magnetic-dipole, magnetic-quadrupole, and spin-forbidden transitions from the ground state ($3p^6\ ^1S_0$), respectively.

Peak		*JL* designation	Intermediate coupling	Tran.	*E* (eV) COWAN	*E* (eV) Moore
		$3p^5 3d[1/2]_1$	$+0.9662(3p^5 3d\ ^3P_1)-0.1119(3p^5 5s\ ^1P_1)$ $+0.1147(3p^5 3d\ ^1P_1)-0.1216(3p^5 4d\ ^3P_1)$	E_1	13.908	13.864
	F_1	$3p^5 3d[7/2]_3$	$0.8752(3p^5 3d\ ^3F_3)-0.2118(3p^5 3d\ ^1F_3)$ $+0.2880(3p^5 3d\ ^3D_3)$	E_3	14.007	14.013
	F_2	$3p^5 5s[3/2]_1$	$0.7485(3p^5 5s\ ^1P_1)-0.6588(3p^5 5s\ ^1P_3)$	E_1	14.109	14.090
F	F_3	$3p^5 3d[5/2]_3$	$0.4464(3p^5 3d\ ^3F_3)+0.6908(3p^5 3d\ ^1F_3)$ $-0.5682(3p^5 3d\ ^3D_3)$	E_3	14.089	14.099
	F_4	$3p^5 3d[3/2]_1$	$-0.1452(3p^5 3d\ ^3P_1)+0.8941(3p^5 3d\ ^1D_3)$ $+0.4147(3p^5 3d\ ^1P_1)$	E_1	14.170	14.153
		$3p^5 3d[5/2]_2$	$0.8073(3p^5 3d\ ^3F_2)+0.5855(3p^5 3d\ ^1D_2)$	M_2	14.056	14.063
		$3p^5 5s[3/2]_2$	$0.9668(3p^5 5s\ ^3D_2)$	T	14.090	14.068
		$3p^5 3d'[5/2]_2$	$0.1862(3p^5 3d\ ^3P_2)-0.4546(3p^5 3d\ ^3F_2)$ $0.6253(3p^5 3d\ ^1D_2)-0.5940(3p^5 3d\ ^3D_2)$	M_2	14.199	14.214
		$3p^5 3d[3/2]_2$	$-0.2286(3p^5 3d\ ^3P_2)-0.3714(3p^5 3d\ ^3F_2)$ $+0.1215(3p^5 5s\ ^3P_2)+0.5097(3p^5 3d\ ^1D_2)$ $+0.7281(3p^5 3d\ ^3D_2)$	M_2	14.199	14.214
	G_1	$3p^5 3d'[5/2]_3$	$-0.1769(3p^5 3d\ ^3F_3)+0.6897(3p^5 3d\ ^1F_3)$ $+0.6990(3p^5 3d\ ^3D_3)$	E_3	14.218	14.236
G	G_2	$3p^5 5s[1/2]_1$	$0.1326(3p^5 3d\ ^3P_1)+0.6506(3p^5 5s\ ^1P_1)$ $+0.7439(3p^5 5s\ ^3P_1)$	E_1	14.266	14.255
	G_3	$3p^5 3d'[3/2]_1$	$-0.4053(3p^5 3d\ ^3D_1)+0.8403(3p^5 3d\ ^1P_1)$ $-0.1266(3p^5 4d\ ^3D_1)+0.1175(3p^5 4d\ ^1P_1)$	E_1	14.349	14.304
		$3p^5 5s'[1/2]_0$	$0.9927(3p^5 5p\ ^3P_0)$	T	14.252	14.241
	H_1	$3p^5 5p[5/2]_2$	$0.6729(3p^5 5p\ ^1D_2)+0.4443(3p^5 5p\ ^3P_2)$ $-0.5914(3p^5 5p\ ^3D_2)$	E_2	14.508	14.506
H	H_2	$3p^5 5p[3/2]_2$	$-0.1675(3p^5 5p\ ^1D_2)+0.8698(3p^5 5p\ ^3P_2)$ $+0.4628(3p^5 5p\ ^3D_2)$	E_2	14.529	14.529
	H_3	$3p^5 5p[1/2]_0$	$0.8283(3p^5 5p\ ^3P_0)+0.5587(3p^5 5p\ ^1S_0)$	E_0	14.592	14.576
		$3p^5 5p[5/2]_3$	$0.9997(3p^5 5p\ ^3D_3)$	T	14.501	14.499
		$3p^5 5p[1/2]_1$	$0.9030(3p^5 5p\ ^3S_1)+0.4157(3p^5 5p\ ^3P_1)$	$M1$	14.475	14.464
		$3p^5 5p[3/2]_1$	$0.2322(3p^5 5p\ ^3S_1)+0.7184(3p^5 5p\ ^1P_1)$ $+0.4239(3p^5 5p\ ^3D_1)-0.4989(3p^5 5p\ ^3P_1)$	M_1	14.526	14.525
		$3p^5 5p'[3/2]_1$	$-0.4803(3p^5 5p\ ^1P_1)+0.8750(3p^5 5p\ ^3D_1)$	M_1	14.672	14.681
		$3p^5 5p'[1/2]_1$	$-0.3499(3p^5 5p\ ^3S_1)+0.5021(3p^5 5p\ ^1P_1)$ $+0.2304(3p^5 5p\ ^3D_1)+0.7554(3p^5 5p\ ^3P_1)$	M_1	14.679	14.687
	I_1	$3p^5 5p'[3/2]_2$	$0.7203(3p^5 5p\ ^1D_2)-0.2125(3p^5 5p\ ^3P_2)$ $+0.6598(3p^5 5p\ ^3D_2)$	E_2	14.679	14.688
	I_2	$3p^5 4d[1/2]_1$	$0.9437(3p^5 4d\ ^3P_1)+0.1846(3p^5 4d\ ^3D_1)$ $+0.1585(3p^5 4d\ ^1P_1)-0.1379(3p^5 5d\ ^3P_1)$	E_1	14.756	14.711
I	I_3	$3p^5 5p'[1/2]_0$	$-0.1870(3p^5 4p\ ^1S_0)-0.5329(3p^5 5p\ ^3P_0)$ $+0.7821(3p^5 5p\ ^1S_0)-0.1524(3p^5 6p\ ^3P_0)$	E_0	14.753	14.738
	I_4	$3p^5 4d[7/2]_3$	$0.8170(3p^5 4d\ ^3F_3)-0.1566(3p^5 4d\ ^3D_3)$ $-0.5435(3p^5 4d\ ^1F_3)$	E_3	14.793	14.781

dipole transition to $3d[1/2]_1$ was too low to be observed because of the very low value of the singlet component shown in Table I. Based upon above discussion, the transition multipolarities for *F*–*I* were assigned and shown in Table I.

In the following we will discuss the GOS's for the valence-shell excitations of Ar (the data are shown in Table II). First, we will discuss the dipole-allowed transitions. The present GOS's of the electric-dipole transitions to $3d[3/2]_1$ and $3d'[3/2]_1$ are shown in Figs. 3 and 4. It can be seen that

TABLE II. The GOS's for the excitations to $3p^5(3d,3d',5p,5p',5s,4d)$. The numbers in square brackets denote the power of 10.

K^2	$3d[3/2]_1$	$3d'[3/2]_1$	$5p[1/2]_0$	$5p[5/2]_2+5p[3/2]_2$	$3d[7/2]_3$
0.019	7.94[−2]	9.67[−2]	1.60[−3]	4.54[−4]	
0.061	6.43[−2]	7.64[−2]	1.94[−3]	1.15[−3]	
0.13	5.17[−2]	6.29[−2]	3.79[−3]	1.98[−3]	
0.23	4.35[−2]	4.98[−2]	3.58[−3]	2.65[−3]	2.09[−4]
0.35	2.65[−2]	3.34[−2]	3.57[−3]	2.69[−3]	8.84[−4]
0.51	1.77[−2]	2.22[−2]	3.16[−3]	2.33[−3]	1.37[−3]
0.69	1.10[−2]	1.35[−2]	2.95[−3]	2.37[−3]	1.61[−3]
0.90	5.44[−3]	6.51[−3]	2.34[−3]	1.79[−3]	2.15[−3]
1.14	3.01[−3]	2.93[−3]	1.92[−3]	5.26[−4]	1.89[−3]
1.40	2.24[−3]	2.19[−3]	1.49[−3]	4.35[−4]	1.72[−3]
1.69	1.91[−3]	1.94[−3]	7.63[−4]	1.83[−4]	1.29[−3]
2.01	1.61[−3]	2.05[−3]	5.94[−4]	1.95[−4]	1.27[−3]
2.36	1.57[−3]	1.91[−3]	4.07[−4]	1.27[−4]	9.08[−4]
2.74	1.20[−3]	1.45[−3]	3.36[−4]	2.52[−4]	5.16[−4]
3.14	9.71[−4]	1.62[−3]	4.22[−4]	6.21[−5]	6.12[−4]
3.57	1.03[−3]	1.09[−3]	3.51[−4]	1.42[−4]	3.04[−4]
4.03	7.04[−4]	7.47[−4]	2.08[−4]	9.39[−5]	2.25[−4]
K^2	$4d[7/2]_3$	$5s[3/2]_1+3d[5/2]_3$	$3d'[5/2]_3+5s[1/2]_1$	$5p'[3/2]_2+4d[1/2]_1+5p[1/2]_0$	
0.01		2.59[−2]	9.51[−3]	2.99[−3]	
0.06		2.21[−2]	7.61[−3]	4.12[−3]	
0.13		2.03[−2]	7.52[−3]	5.67[−3]	
0.23	1.02[−5]	1.63[−2]	4.79[−3]	5.52[−3]	
0.35	5.28[−4]	1.11[−2]	2.96[−3]	5.52[−3]	
0.51	1.12[−3]	9.06[−3]	3.07[−3]	5.10[−3]	
0.69	8.32[−4]	7.08[−3]	4.12[−3]	4.59[−3]	
0.90	2.07[−3]	6.81[−3]	3.73[−3]	2.36[−3]	
1.14	1.77[−3]	5.78[−3]	3.45[−3]	1.39[−3]	
1.40	2.03[−3]	5.30[−3]	3.69[−3]	6.80[−4]	
1.69	1.36[−3]	3.63[−3]	2.21[−3]	2.24[−4]	
2.01	1.48[−3]	3.55[−3]	2.35[−3]	2.70[−4]	
2.36	1.25[−3]	2.36[−3]	1.36[−3]	4.40[−4]	
2.74	7.80[−4]	2.05[−3]	1.24[−3]	6.73[−4]	
3.14	8.12[−4]	1.83[−3]	9.92[−4]	1.67[−4]	
3.57	5.09[−4]	1.20[−3]	6.93[−4]	2.34[−4]	
4.03	3.88[−4]	8.80[−4]	6.03[−4]	1.98[−4]	

their GOS's decrease quickly with the increase of momentum transfer in lower K^2 region, which is the typical character of the dipole-allowed transition. It is noticed that GOS of the transition to $3d'[3/2]_1$ has a shoulder at about $K^2=2$ a.u. (see the inset graphs in Fig. 4). The solid lines in Figs. 3 and 4 are the fitted results using the Lassettre formula [35]. The extrapolated optical oscillator strengths (OOS's) are 0.085 and 0.105, which are in agreement with the results of 0.0929 and 0.106 measured by the dipole (e,e) method [36].

Second, we will discuss the dipole-forbidden transitions in $3p\rightarrow 5p$. The GOS's of the electric-monopole transition to $5p[1/2]_0$ are shown in Fig. 5 and compared with the calculated ones using the HF and RPAE methods [26]. The GOS maximum for the electric monopole transition to $5p[1/2]_0$ locates at about $K^2=0.4$ a.u., which is in agreement with the calculated one. However, the present GOS profile is different from the calculated one. It can be seen that the present GOS has a maximum at about $K^2=0.4$ a.u. and a shoulder at about $K^2=3$ a.u.; similar GOS profiles have been observed for the electric-monopole transitions in $3p\rightarrow 4p$ (paper I). However, the theoretical predictions by Amusia *et al.* [26] have only one maximum. Besides, there is an obvious difference in absolute values between present results and the theoretical ones in $K^2<0.3$ a.u. and $1.4<K^2<3$ a.u. It should be emphasized that the present GOS's in the lower K^2 region should have larger errors resulting from the deconvolution

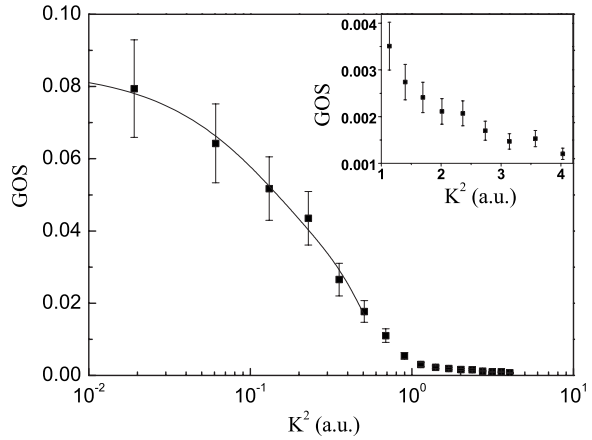

FIG. 3. The GOS's for the excitation to $3d[3/2]_1$ (peak F_4). Solid squares, present results; solid line, present fitted results.

procedure because of the low intensities at small scattering angles.

Figure 6 shows the sum of the GOS's for the electric-quadrupole excitations to $5p[5/2]_2$ and $5p[3/2]_2$ and the comparison with the calculated ones [26]. It can be seen that the GOS maximum locates at about $K^2=0.35$ a.u., which is in agreement with the calculated one. However, it is noticed that the present GOS's profiles are different from the theoretical predictions by Amusia *et al.* [26]. The present GOS's increase more quickly in $K^2<0.13$ a.u. while they decrease more quickly in $K^2>0.9$ a.u. than the calculated ones. Besides, there is large difference between them about the absolute values in the larger K^2 region. This indicates that further experimental and theoretical investigations of the electric-monopole and electric-quadrupole excitations in $3p\rightarrow 5p$ are greatly recommended.

The GOS's for the electric-octupole transitions to $3d[7/2]_3$ and $4d[7/2]_3$ are shown in Figs. 7 and 8, respectively. For the GOS of the excitation to $3d[7/2]_3$, only one maximum locates at about $K^2=1.0$ a.u. Similarly, the GOS of the excitation to $4d[7/2]_3$ has only one maximum, which

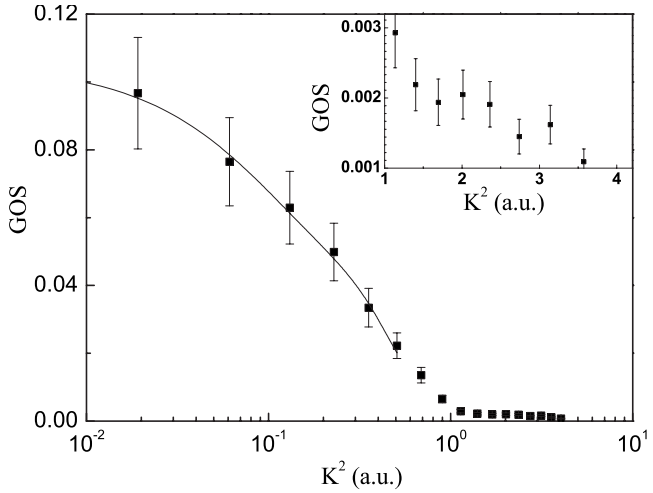

FIG. 4. The GOS for the excitation to $3d'[3/2]_1$ (peak G_3). Solid squares, present results; solid line, present present fitted results.

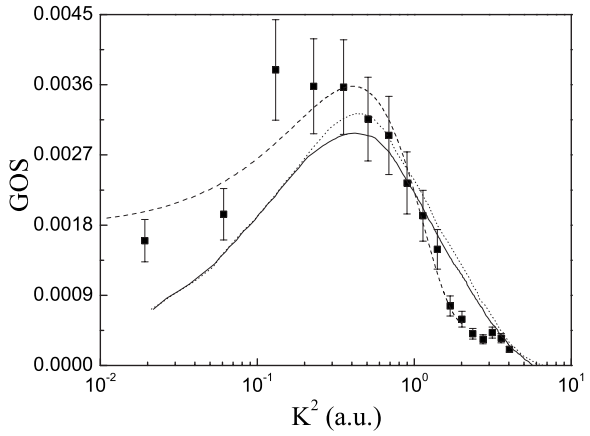

FIG. 5. The GOS for the electric-monopole excitation to $3p^55p[1/2]_0$ (peak H_3). Solid squares, present results; dashed line, present fitted results; solid line, RPAE calculation [26]; dotted line, HF calculation [26]. Here the theoretical calculations are multiplied by the square of the intermediate coupling coefficient of the singlet component $3p^55p^1S_0$ calculated by this work.

locates at about $K^2=1.2$ a.u. There is no theoretical calculations for comparison.

Finally, we will discuss the mixed transitions; each of them contains both dipole-allowed and dipole-forbidden transitions. Figure 9 shows the sum of GOS's for excitations to $5s[3/2]_1$ and $3d[5/2]_3$. It can be seen that the GOS's decrease with increasing of the momentum transfer in the lower-K^2 region, which is the typical character of dipole-allowed transitions; here, the contribution from $5s[3/2]_1$ is dominating. There is a shoulder at about $K^2=1.0$ a.u., which should be due to the excitation to $3d[5/2]_3$ since the GOS for electric-octupole excitation has a maximum around $K^2=1.0$ a.u. The extrapolated OOS for the GOS's is 0.0259, which is in agreement with the result (0.0241) of $5s[3/2]_1$ measured by the dipole (e,e) method [36].

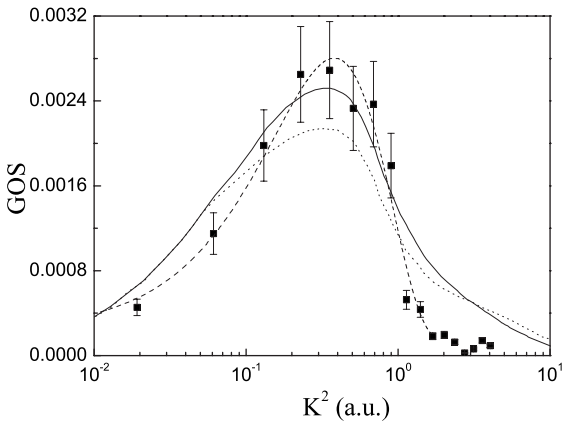

FIG. 6. The sum of GOS's for the electric-quadrupole excitations to $3p^55p[5/2]_2$ and $3p^55p[3/2]_2$ (peaks H_1 and H_2). Solid squares, present results; dashed line, present fitted results; solid line, RPAE calculation [26]; dotted line, HF calculation [26]. Here the theoretical calculations are multiplied by the sum of the squares of the intermediate coupling coefficients of the singlet component $3p^55p^1D_2$ calculated by this work.

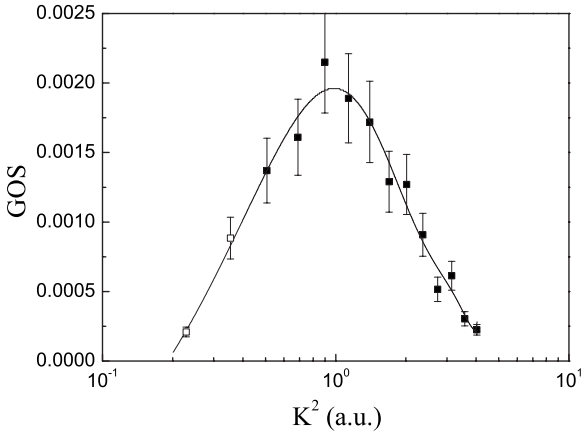

FIG. 7. The GOS for the excitation to $3d[7/2]_3$ (peak F_1). Solid and open squares, present results; the data shown as open squares are less reliable because of the contamination in the deconvolution from the neighboring strong peaks F_2+F_3; solid line, present fitted results.

Figure 10 shows the sum of GOS's for transitions to $3d'[5/2]_3$ and $5s[1/2]_1$. It can be seen that there are a dip at about $K^2=0.4$ a.u. and a shoulder at about $K^2=1.0$ a.u. The decrease with increasing of momentum transfer in lower K^2 is mainly the contribution from the dipole-allowed excitation to $5s[1/2]_1$. The dip is the combined effect of excitations to $3d'[5/2]_3$ and $5s[1/2]_1$ since the GOS for the electric-dipole excitation decreases quickly with increasing of the momentum transfer in the lower-K^2 region, while the GOS for electric-octupole excitation is reverse (see Fig. 7). The shoulder at about $K^2=1.0$ a.u. attributes to the contribution from the excitation to $3d'[5/2]_3$ as discussed above. The extrapolated OOS for the GOS's is 0.0103, which is smaller than the result (0.0122) of $5s[1/2]_1$ measured by the dipole (e,e) method [36]. The difference may be attributed to the errors resulting from the deconvolution and extrapolation procedures.

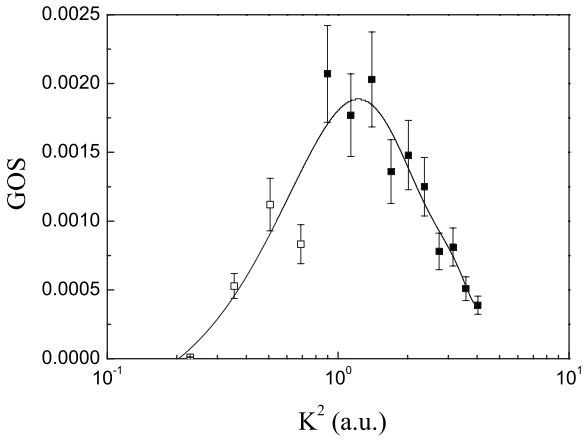

FIG. 8. The GOS for the excitation to $4d[7/2]_3$ (peak I_4). Solid and open squares, present results; the data shown as open squares are less reliable because of the contamination in the deconvolution from the neighboring strong peaks J and $I_1+I_2+I_3$; solid line, present fitted results.

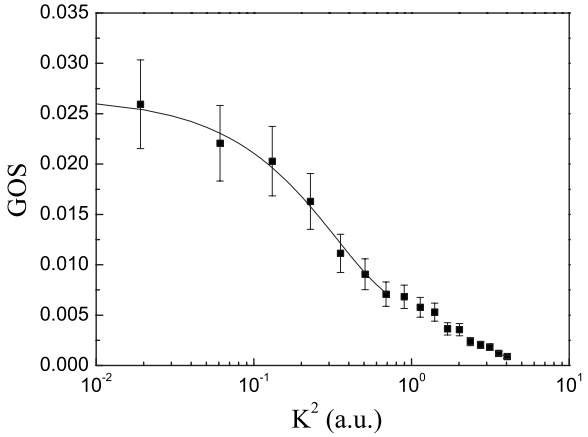

FIG. 9. The GOS for the excitations to $5s[3/2]_1+3d[5/2]_3$ (peak F_2 and F_3). Solid squares, present results; solid line, present fitted results.

It can be seen from Table I that the electric-octupole excitations to $3d[7/2]_3$, $3d[5/2]_3$, and $3d'[5/2]_3$ (peaks $F1$, $F3$, and $G1$) have the same singlet components of $3d\ ^1F_3$ in the intermediate scheme. The intermediate coupling coefficients of $3d\ ^1F_3$ are 0.2118, 0.6908, and 0.6897, respectively. Therefore, the ratio of the GOS's for them should be about $0.2118^2:0.6908^2:0.6897^2\approx 1:11:11$. However, the present experimental ratio is about $0.002:0.007:0.004=2:7:4$ (see Figs. 7, 9, and 10); herein, the contributions from the electric-dipole excitations to $5s[3/2]_1$ and $5s[1/2]_1$ were not taken into account. This shows that the present calculations of intermediate coupling coefficients still need to be improved.

The GOS for the excitations to $5p'[3/2]_2+4d[1/2]_1+5p'[1/2]_0$ is shown in Fig. 11. The extrapolated OOS is 0.0028, which is agreement with the result (0.0025) of $4d[1/2]_1$ measured by the dipole (e,e) method [36].

IV. SUMMARY AND CONCLUSION

The valence-shell excitations of Ar were investigated by an incident electron energy of 2500 eV. The excitations are

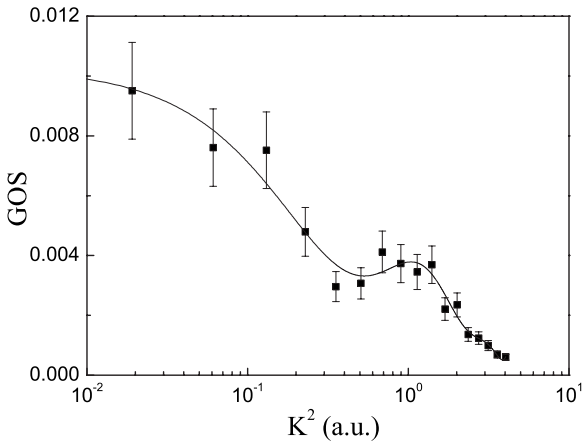

FIG. 10. The GOS for the excitations to $3d'[5/2]_3+5s[1/2]_1$ (peaks G_1 and G_2). Solid squares, present results; solid line, present fitted results.

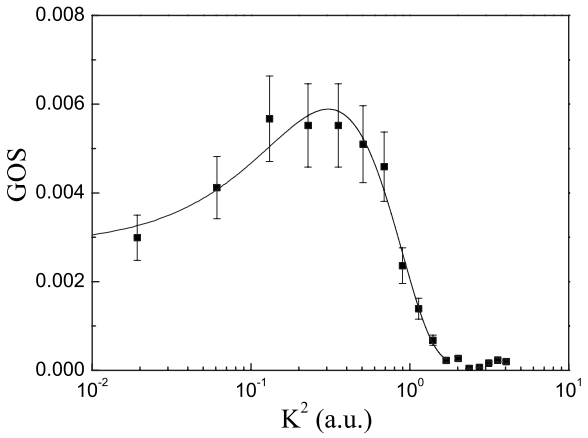

FIG. 11. The GOS for the excitations to $5p'[3/2]_2+4d[1/2]_1+5p'[1/2]_0$ (peaks I_1, I_2, and I_3). Solid squares, present results; solid line, present fitted results.

classified as electric-monopole, electric-dipole, electric-quadrupole, and electric-octupole transitions with the help of our calculated intermediate coupling coefficients. Furthermore, the GOS's for the excitations to $3p^5(3d,3d',5p,5p',5s,4d)$ of Ar have been determined in the K^2 region of 0.019–4.03 a.u. The GOS's for the electric-monopole and electric-quadrupole excitations in $3p\rightarrow 5p$ were compared with the theoretical calculations by Amusia *et al.* [26] with the HF and RPAE methods. The present maximum positions for the electric-monopole and electric-quadrupole excitations in $3p\rightarrow 5p$ are in agreement with the calculated ones [26]. However, the profiles of GOS's have apparent differences between the theoretical calculations and experimental results. Furthermore, the measured GOS ratios (2: 7: 4) for the electric-octupole transitions $3d[7/2]_3$, $3d[5/2]_3$, and $3d'[5/2]_3$ are different from the ones (1: 11: 11) calculated from the present intermediate coupling coefficients. So further theoretical investigations of the electric-monopole, electric-dipole, electric-quadrupole, and electric-octupole excitations are greatly recommended.

ACKNOWLEDGMENTS

Support of this work by the National Nature Science Foundation of China (Grant No. 10474089) is gratefully acknowledged.

[1] H. D. Cheng, L. F. Zhu, X. J. Liu, Z. S. Yuan, W. B. Li, and K. Z. Xu, Phys. Rev. A **71**, 032714 (2005).
[2] H. D. Cheng, L. F. Zhu, Z. S. Yuan, X. J. Liu, J. M. Sun, W. C. Jiang, and K. Z. Xu, Phys. Rev. A **72**, 012715 (2005).
[3] L. F. Zhu, H. D. Cheng, Z. S. Yuan, X. J. Liu, J. M. Sun, and K. Z. Xu, Phys. Rev. A **73**, 042703 (2006).
[4] C. C. Turci, J. T. Francis, T. Tyliszczak, G. G. de Souza, and A. P. Hitchcock, Phys. Rev. A **52**, 4678 (1995).
[5] X. J. Liu, L. F. Zhu, Z. S. Yuan, W. B. Li, H. D. Cheng, Y. P. Huang, Z. P. Zhong, K. Z. Xu, and J. M. Li, Phys. Rev. Lett. **91**, 193203 (2003).
[6] Y. K. Kim, M. Inokuti, G. E. Chamberlain, and S. R. Mielczarek, Phys. Rev. Lett. **21**, 1146 (1968).
[7] P. Molaro, S. A. Levshakov, S. D'Odorico, P. Bonifacio, and M. Centurión, Astrophys. J. **549**, 90 (2001).
[8] K. W. Jalufka, R. J. Deyoung, F. Hohl, and M. D. Williams, Appl. Phys. Lett. **29**, 188 (1976).
[9] K. Z. Xu, R. F. Feng, S. L. Wu, Q. Ji, X. J. Zhang, Z. P. Zhong, and Y. Zheng, Phys. Rev. A **53**, 3081 (1996).
[10] W. B. Li, L. F. Zhu, X. J. Liu, Z. S. Yuan, J. M. Sun, H. D. Cheng, Z. P. Zhong, and K. Z. Xu, Phys. Rev. A **67**, 062708 (2003).
[11] W. C. Tam and C. E. Brion, J. Electron Spectrosc. Relat. Phenom. **2**, 111 (1973).
[12] B. R. Lewis, E. Weigold, and P. J. O. Teubner, J. Phys. B **8**, 212 (1975).
[13] A. Chutjian and D. C. Cartwright, Phys. Rev. A **23**, 2178 (1981).
[14] D. M. Filipović, B. P. Marinković, V. Pejčev, and L. Vučković, J. Phys. B **33**, 677 (2000).
[15] D. M. Filipović, B. P. Marinković, V. Pejčev, and L. Vučković, J. Phys. B **33**, 2081 (2000).
[16] M. A. Khakoo, P. Vandeventer, J. G. Childers, I. Kanik, C. J. Fontes, K. Bartschat, K. Bartschat, V. Zeman, D. H. Madison, S. Saxena, R. Srivastava, and A. D. Stauffer, J. Phys. B **37**, 247 (2004).
[17] G. P. Li, T. Takayanagi, K. Wakiya, H. Suzuki, T. Ajiro, S. Yagi, S. S. Kano, and H. Takuma, Phys. Rev. A **38**, 1240 (1988).
[18] C. E. Bielschowsky, G. G. B. de Souza, C. A. Lucas, and H. M. Boechat Roberty, Phys. Rev. A **38**, 3405 (1988).
[19] Q. Ji, S. L. Wu, R. F. Feng, X. J. Zhang, L. F. Zhu, Z. P. Zhong, K. Z. Xu, and Y. Zhang, Phys. Rev. A **54**, 2786 (1996).
[20] X. W. Fan and K. T. Leung, Phys. Rev. A **62**, 062703 (2000).
[21] T. C. Wong, J. S. Lee, and R. A. Bonham, Phys. Rev. A **11**, 1963 (1975).
[22] R. A. Bonham, J. Chem. Phys. **36**, 3260 (1962).
[23] I. Shimamura, J. Phys. Soc. Jpn. **30**, 824 (1971).
[24] Z. F. Chen, A. Z. Msezane, and M. Y. Amusia, Phys. Rev. A **60**, 5115 (1999).
[25] L. R. Peterson and J. E. Allen, Jr., J. Chem. Phys. **56**, 6068 (1972).
[26] M. Y. Amusia, L. V. Chernysheva, Z. Felfli, and A. Z. Msezane, Phys. Rev. A **67**, 022703 (2003).
[27] M. Inokuti, Rev. Mod. Phys. **43**, 297 (1971).
[28] H. Bethe, Ann. Phys. **5**, 325 (1930); , Z. Phys. **76**, 293 (1930).
[29] B. G. Tian and J. M. Li, Acta Phys. Sin. **33**, 1401 (1984).
[30] J. J. Abdallah, R. E. H. Clark, and R. D. Cowan (unpublished).
[31] C. E. Moore, *Atomic Energy Levels*, Natl. Bur. Stand. (U. S.) Circ. No. 467 (U.S. GPO, Washington, D.C., 1971), Vol. 2.
[32] R. E. H. Clark, J. Abdallah, Jr., G. Csanak, and S. P. Kramer, Phys. Rev. A **40**, 2935 (1989).

[33] R. E. H. Clark, G. Csanak, and J. Abdallah, Jr., Phys. Rev. A **44**, 2874 (1991).

[34] R. D. Cowan, *The Theory of Atomic Structure and Spectra* (University of California Press, Berkeley, CA, 1981).

[35] E. N. Lassettre, J. Chem. Phys. **43**, 4479 (1965); K. N. Klump and E. N. Lassettre, *ibid.* **68**, 886 (1978).

[36] S. L. Wu, Z. P. Zhong, R. F. Feng, S. L. Xing, B. X. Yang, and K. Z. Xu, Phys. Rev. A **51**, 4494 (1995).